



Article

Disconnected Flows, Eroded Landscapes: A Case Study of Human Impact on a Judean Desert Water System

Nurit Shtober-Zisu ^{1,*}  and Boaz Zissu ² ¹ School of Environmental Sciences, University of Haifa, 199 Abba Khoushi Ave., Haifa 3498838, Israel² The Martin (Szusz) Department of Land of Israel and Archaeology, Bar-Ilan University, Ramat Gan 5290002, Israel; boaz.zissu@biu.ac.il

* Correspondence: nshtober@research.haifa.ac.il

Abstract: The Bir el-Umdan cistern, a prominent archaeological site in the Judean Desert, is one of the largest and best preserved water systems in the region. Hewn in chalk, the cistern area measures 114 m² and has a ~700 m³ volume. Two massive columns, each with a base diameter of 2.5 m, support the ceiling within the cistern's interior. This impressive structure is estimated to date back to the Hellenistic to Late Antiquity periods based on its architectural characteristics. Historical records indicate that the cistern was documented on 19th-century maps but disappeared from the 1935 and 1943 British Mandate maps. Its reappearance on the 1967 Survey of Israel map includes an upstream road disconnecting the cistern from its natural drainage basin. Despite its renovation in the 2010s, the cistern's water supply remains limited due to its reduced catchment area, which now constitutes only 25% of its original size. Runoff coefficients calculated for the cistern's drainage basin are relatively low (1.4% to 8.1%) compared to other desert regions. We analyzed the 21st-century runoff coefficient and recurrence interval over the original drainage basin (0.12 km²) to estimate the water volumes in antiquity. Our analysis suggests that using an 8.1% runoff coefficient, the estimated water volume is 806 m³, implying a cistern overflow every 6–7 years. A more conservative estimate using a 5% runoff coefficient yields a water volume of 500 m³ and a 15-year recurrence interval. Sediment analysis reveals that silt particles dominate the sediment accumulated in the cistern and its upstream sedimentation basins. The consistent grain size distribution throughout the system indicates rapid water flow during flood events. Reconstructing the sedimentation history is challenging due to potential maintenance and possible dredging and cleaning operations.



Citation: Shtober-Zisu, N.; Zissu, B. Disconnected Flows, Eroded Landscapes: A Case Study of Human Impact on a Judean Desert Water System. *Land* **2024**, *13*, 1679. <https://doi.org/10.3390/land13101679>

Academic Editor: Nick B. Comerford

Received: 4 September 2024

Revised: 29 September 2024

Accepted: 10 October 2024

Published: 15 October 2024



Copyright: © 2024 by the authors. Licensee MDPI, Basel, Switzerland. This article is an open access article distributed under the terms and conditions of the Creative Commons Attribution (CC BY) license (<https://creativecommons.org/licenses/by/4.0/>).

Keywords: disconnectivity; runoff coefficient; rainfall/runoff relation; Hellenistic period; Late Antiquity; water system; Judean Desert; Bir el-Umdan cistern

1. Introduction

Hydrological disconnectivity refers to the fragmentation of the continuity of water pathways for water flow, hindering runoff and sediment movement, in contrast to hydrological connectivity, which is essential for efficient water and sediment transfer. This phenomenon is critical in understanding landscape degradation, particularly in arid and semi-arid regions where water scarcity can lead to significant geomorphological and ecological changes [1]. Hydrological connectivity is the result of a complex interaction between various environmental factors such as geology, topography, climate, soil, flora and fauna, as well as human activity, for example, [2–6]. These factors influence the movement of water and sediment in different environmental conditions and geomorphic processes, in a variety of landforms such as rivers, hillsides, coastal areas/deltas, as well as aeolian landscapes and other environments [7]. The degree of connectivity along hillslopes, at the hillslope–channel interface, and along streams affects water resource redistribution, sediment movement, and biological fluxes [8]. Furthermore, the dynamic connectivity behavior of surface runoff in response to rainfall events is influenced by the spatial heterogeneity of topography and

surface properties, highlighting the importance of understanding how different parts of a hydrological system connect through fluxes across time and space in the landscape [9]. Human intervention in river systems often disrupts the natural hydro-geomorphic connectivity of meteoric water flow and sediment transport [10–12]. This disruption occurs when dams and reservoirs obstruct the river flow [13], when the river is channelized [14,15], or when there are changes in land use and land cover [16]. These activities collectively alter the hydrological and ecological dynamics of these systems.

In the long run, the cumulative effects of land use changes have been shown to exceed those of climate change, fundamentally altering river morphology and stratigraphy [17]. These changes can lead to irreversible species losses and shifts in community composition, further destabilizing ecosystem health [18].

This article examines a small ephemeral stream in the Judean Desert that was disconnected during antiquity when three water cisterns were constructed within its channel, and then again in the 20th century when a newly built road blocked the water flow into the cisterns and led to significant hydrological and geomorphological changes.

Humans have inhabited the Judean Desert since prehistoric times [19]. From the Chalcolithic to the Early Arab period [20–22], the Judean Desert had always attracted human habitation and activity due to its strategic location and the presence of oases and water resources. Remains of extensive human activity from various periods have been discovered on the western shores of the Dead Sea. For example, an isolated temple from the Chalcolithic period was found at En Gedi, continuing with the development of the site into an industrial center during the Iron Age, and culminating in its transformation into of a large Jewish village during the Roman and Byzantine periods [23]. Due to its proximity to the central mountainous country, the Judean Desert served as the “backyard” of more favorable environments. It often provided temporary residence for nomads, or refuge for rebels and other social and religious groups that sought an isolated location [24].

Desert transportation routes in the Judean Desert were determined mainly by the terrain, local conditions, and water availability, resulting in scattered, narrow paths primarily used by nomadic herders. The most extensive road development in the Judean Desert and the Dead Sea regions occurred during the Roman period [25], demonstrating an intimate knowledge of the land and advanced technical capabilities. These roads were often accompanied by water cisterns, guard stations, and stops [26].

In the harsh, arid environmental conditions of the Judean Desert, human survival has necessitated extensive efforts to secure the water required for drinking and food production, often relying on rainwater. Rainwater harvesting emerges as a viable strategy when droughts pose a recurring threat and significantly impact economic stability or food security under traditional rainfall-dependent farming. Increasing the available water supply beyond natural precipitation becomes essential in such circumstances, and rainwater harvesting systems could bridge this water deficit for agricultural purposes [27]. Water availability was important not just for the inhabitants’ daily needs but also for watering the herds of animals. The collection and storage of water was achieved by excavating and plastering cisterns, reinforcing channels to guide runoff from sloped areas into these cisterns, and constructing dams to redirect winter flows [28–30]. Bruins [27] defined three main types of runoff collecting systems in the Negev: (1) terraced wadi system, (2) hillside conduit system, and (3) diversion system. The first two systems were constructed mainly in small basins of low orders (first to fourth) and are discussed in the present study; the third one was constructed in higher basin orders (fifth to seventh) and floodplains adjacent to the main channel [31].

Archaeological evidence dating back to the Iron Age indicates that reliable rainwater-harvesting agricultural systems were established in some parts of the Judean Desert [32,33], suggesting that these systems supported permanent farming settlements, which primarily relied on runoff farming over alluvial soils. Gibson et al. [34] propose a different scenario for the northeastern Judean Desert during the 7th and early 6th centuries BCE, claiming that pastoralists primarily inhabited this region. Unlike nomadic groups, these pastoralists

held land ownership and property rights, including access to water sources such as water pits and cisterns, indispensable for the survival of their herds.

This study aims to investigate the effects of human intervention on the disconnectivity of a small drainage basin system in the Judean Desert, especially on the rainfall/runoff relationship, water availability, and sedimentation effects on water quality. It is hypothesized that human-induced modifications to the natural drainage system have significantly altered hydrological connectivity, leading to changes in the rainfall–runoff–sediment relationships affecting the availability and quality of water. This study presents important insights into the impact of human development and associated interference on the natural system and water availability. The findings provide a valuable understanding for evaluating the sustainability of rural development projects in dryland environments.

2. Study Area

The Judean Desert is a narrow, north–south trending strip located between the Judean Mountains to the west and the Jordan Rift Valley and the Dead Sea to the east, approximately 80 km long and 20–25 km wide. While the Judean Hills ascend to 800–1000 m elevations, the Dead Sea lies about 430 m below sea level, resulting in a dramatic elevation difference. This pronounced topographic gradient creates a rain-shadow effect, causing a steep decline in annual rainfall from the Judean Mountains of the Mediterranean environment with ~700 mm/yr, to less than 50 mm/yr along the Dead Sea, and a steep increase in average temperatures [35,36].

Recent discoveries in the Judean Desert have unveiled a remarkable hydrological infrastructure that attracted considerable public attention since 2020. Three large cisterns, distanced ~50–70 m from each other, exhibiting distinctive Hellenistic to Late Antiquity architectural characteristics [37], were hewn into the chalk bedrock of the upper Gorfán Stream (Figure 1). The cisterns are located in the channel to collect floodwater, therefore disconnecting the upper and lower reaches of the channel [38]. Changes made to the basin during the 20th and 21st centuries disrupted the hydro-geomorphic connectivity, further attenuating water and disturbing sediment transport. While access to two of these cisterns remains restricted, the accessible third cistern offers insights into the complex interplay between rainfall, runoff, and sedimentation processes in a disconnected catchment.

The cistern, named Bir el-Umdan (“The pillar’s cistern”) by the local population, is located in the Judean Desert at 31°39′57.5″ N, 35°19′17.9″ E. The exposed rock units in the drainage basins consist mainly soft carbonate rocks, comprising three geological units (from top to bottom): (1) the Hatrurim Formation (or the “Mottled Zone”, mz), composed mainly of high-temperature–low-pressure metamorphic minerals, a product of combustion of the bituminous Maastrichtian to Paleocene chalk and marls of the (2) Ghareb (Kug) and Taqiye formations (Figure 1c; [40]), in which the cistern was cut. The third unit, the Mishash Formation (Kumi), comprises massive brecciated brown chert or alternating beds of chalk and chert. This unit also includes massive brown chert and flint with silicified chalk and some phosphorite beds [41,42].

The climate is arid, with a prominent rainy season that extends from October to April, with peak precipitation concentrated in January and February. Generally, rainfall is characterized by short, intense frontal events, deriving from (1) Mediterranean Cyclones during winter [43], (2) Active Red Sea trough, the synoptic system responsible for most flash floods [44], and (3) Tropical Plumes, typically accompanied by a subtropical jet streak [45]. The latter is usually characterized by the development of intense flash floods. The rainfall events are interspersed with extended dry periods, marked by pronounced seasonal fluctuations of cyclical droughts and wet periods.

The average annual rainfall in the cistern area is between 200 and 250 mm/yr, and the average annual temperature is 20 °C (<https://ims.gov.il/he/ClimateAtlas>, accessed on 1 September 2024). Nahal Gorfán stream, like other Judean Desert streams, is characterized by prolonged periods with no flow punctuated by sudden, high-intensity rainfall events during the wet season, resulting in rapid runoff and flash flooding [46]. The soils have

limited agricultural potential and only support very sparse natural vegetation. Soil is light yellowish brown leptosol, calcareous, loamy with 20% clay [47]. The vegetation is dominated by an *Anabais articulata*–*Agathophora alopecuroides* association, accompanied by *Salsola vermiculata* and *Reaumuria hirtella* [48].

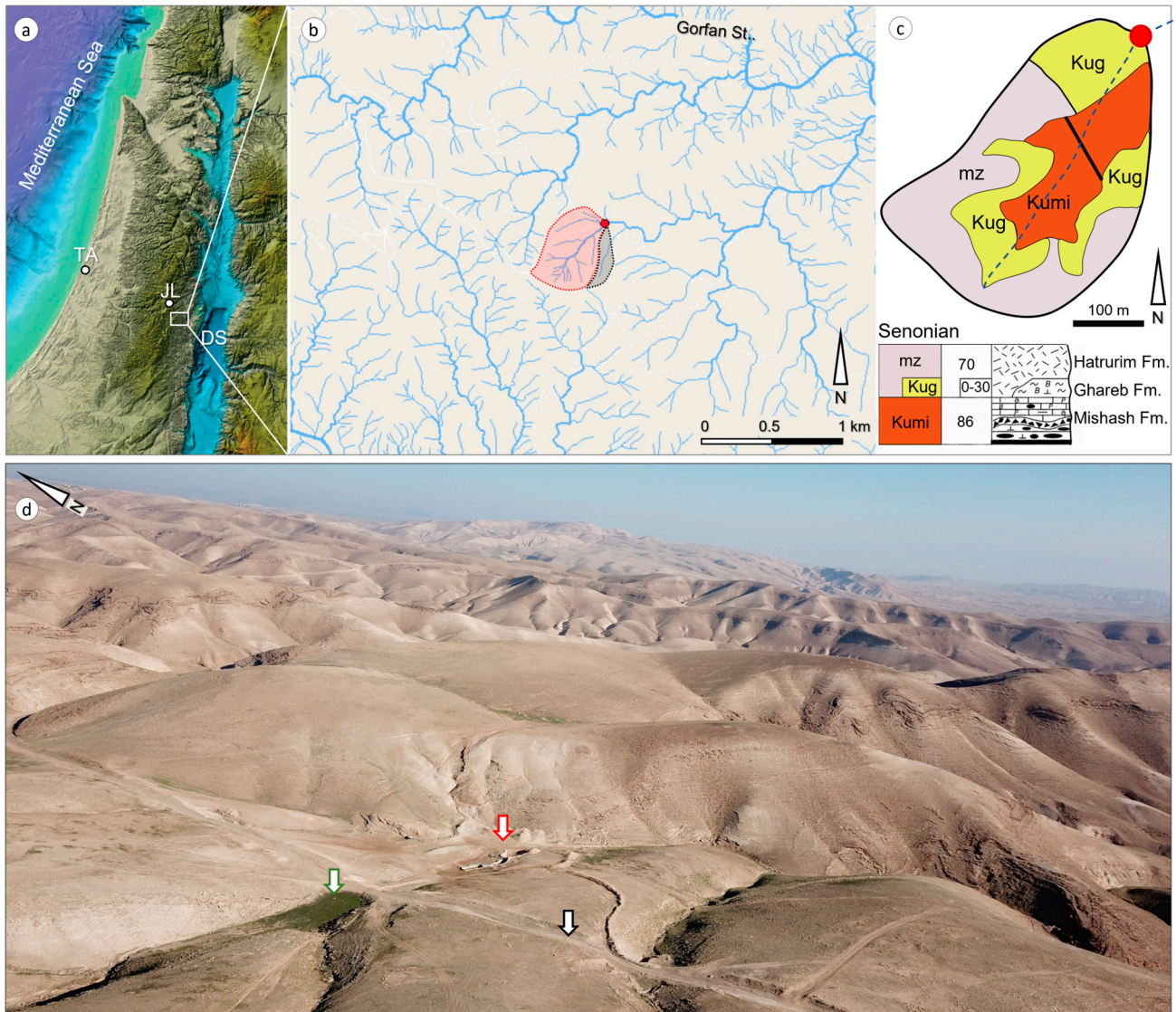


Figure 1. (a) Shaded relief map of the Levant: TA–Tel Aviv, JL–Jerusalem, DS–Dead Sea; (b) regional hydrological drainage net of the studied area with the specific drainage basin of the Bir el-Umdan cistern (red), neighbor drainage basin connected in 2010 (black); (c) geological map and section of the drainage basin, after [39]; (d) aerial photo of the Judean Desert and study site (red arrow). Note the road (black arrow) and the vegetated alluvial fan (green arrow) dammed by the road.

3. Materials and Methods

Data on the cistern and the adjacent slopes were collected through field surveys and mapping, coupled with field observations and comprehensive descriptions that were carried out during several campaigns in 2022. First, a drone survey of the catchment was employed, and subsequently, the cistern was scanned using a Lidar app available on iPhone 14Pro.

We compared the field observations with aerial photographs obtained in 1945 (PS; [49]) and drone photographs from 2022 that were then used to create a detailed basin map.

Additionally, SWP (Survey of Western Palestine) maps [50], British Mandate maps (1935, 1943; [51]), and modern maps [52] were examined.

This dataset was augmented by Citizen Science, a collaborative research approach where members of the public participate in scientific investigations. Extensive information was gathered from hikers, bloggers, and travelers who documented their visits to the cistern on digital and social media, especially on Facebook and Instagram. About 30 of their photographs, accompanied by dates, enabled a four-year reconstruction (2020–2024) of water levels in the cistern (e.g., Figure 2). Water volume in the cistern was calculated by comparing the water levels in the photos with the water marks on the cistern wall. The reconstructed water levels were then incorporated into the daily rainfall data collected by the Israel Meteorological Service (IMS) gauging station situated at Maàle Amos ($31^{\circ}35'44.7''$ N $35^{\circ}13'50.6''$ E), located 11.5 km southwest. The average annual rainfall in Maàle Amos is 276 mm (1991–2020; [53]), which is ~25% higher than at the cistern site.



Figure 2. Variability of the water level in the cistern as pictured in November 2020 (left), when the water depth was ca. 100 cm, and January 2022 (right), when the cistern floor was dry. The photos were retrieved from Instagram (<https://www.instagram.com/gili.shani/>, accessed on 1 September 2024). Publication courtesy of Gili Shani (<https://yoga-gili.com/>, accessed on 1 September 2024).

Ten sediment samples from the slopes, the sedimentary basins, and the cistern floor, each weighing 50 g, were analyzed using the hydrometer method to determine particle size distribution at the Agricultural Research laboratory, Neve Yaàr Research Center. Aggregates were dissolved using Calgon solution (15 mL of 10% Calgon into 400 mL desalinated water) to isolate the mineral fraction; carbonates were left intact. Clay, silt, and sand sizes were defined following the USGS system [54].

4. Results

4.1. Hydrological Infrastructure of the Bir el-Umdan Cistern

Bir el-Umdan cistern is one of the largest and most exceptional examples among hundreds and perhaps thousands of other rock-cut cisterns in the Judean Desert. The cistern is part of a hydrological system that includes both an external filtration component and a subterranean hewn cistern (Figure 3). The external component consists of six constructed basins, each measuring 1–2 m long, designed to slow down the water velocity, enable sedimentation and filter the captured floodwater (Figures 3a,c and 10). In Figure 3a, the uppermost basin is a shallow depression dug within the channel, through which water

flows into the next five smaller basins. The filtered water is eventually conveyed into the underground cistern.

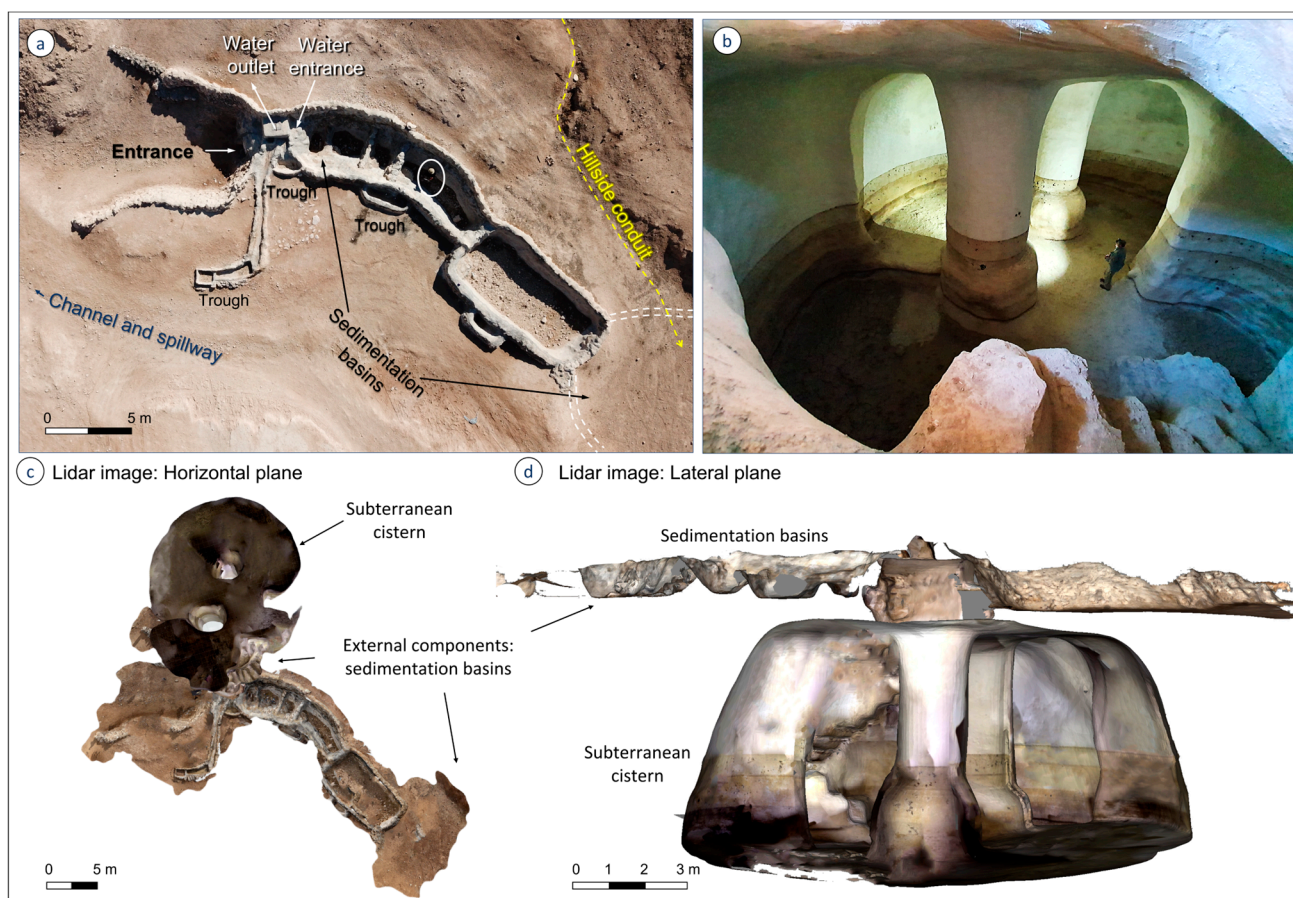


Figure 3. Bir el-Umdan water system: (a) aerial photo of the upper components of the system: six sedimentation basins constructed to catch the coarse sediments, three troughs to water the herds, part of the hillside conduit, channel and spillway. The upper sedimentation basin is delineated by a double white dashed line, indicating a small depression without surrounding construction. Water enters the cistern after filtration and exits only by manual extraction with a bucket through the outlet opening in the cistern's roof. Human for scale, encircled white; (b) the underground cistern, freshly plastered and painted. Note the water levels on the walls. (c,d) Lidar images in horizontal and lateral planes, showing the relations between the subaerial and subterranean components of the Bir system. Three-dimensional scan prepared by Dr. Danny Bickson.

The underground component includes a sub-rounded cistern, hewn in the impermeable chalk of the Ghareb Formation, and plastered to prevent water leakage. It is 6–7 m high, with a basal area of 114 m², and a capacity of ~700 m³ (Figure 3b,d). Two large pillars with a base diameter of 2.5 m support the ceiling, and ten rock-cut steps lead from the entrance to the bottom of the cistern. The thickness of the rock layers above the cistern is ~70–80 cm.

The cistern is located in the channel of a 3rd-order stream, a tributary of the Gorfán-Kidron river system, draining to the Dead Sea (Figure 1b). At the time of construction, it was fed by direct floodwater supplied during the rainy season. The cistern's natural drainage area extends over 0.12 km², and the channel slope is 13.8% (Figures 3 and 4). Nowadays, a hillside conduit directs runoff from the adjacent watershed (0.03 km²) and conveys it into the upper sedimentation basin (Figure 3a).

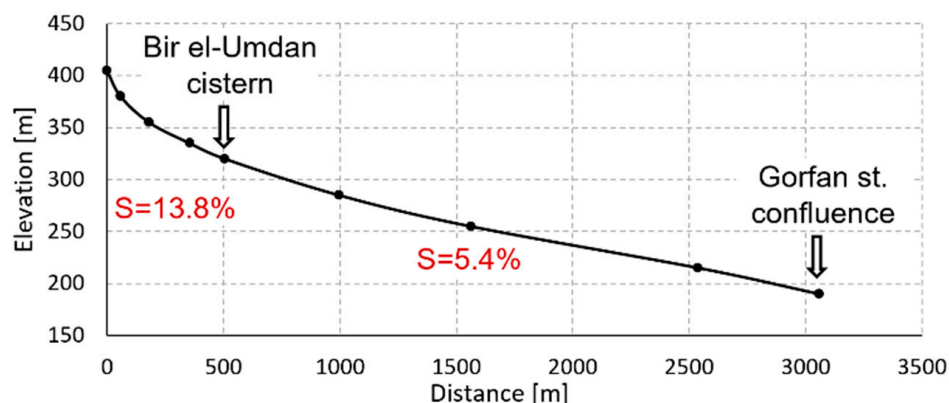


Figure 4. Longitudinal profile of the Bir el-Umdan channel up to the Gorfan stream confluence (see also Figure 1b).

The exact age of the cistern remains uncertain due to the removal and subsequent loss of archaeological artifacts and the application of a thick layer of modern plaster/mortar during a renovation project in the 2010s. This project also involved excavating the area around the cistern, which destroyed any remaining archaeological context. However, based on typological similarities with cisterns from the Negev and other desert regions, it is reasonable to suggest that this cistern was likely constructed during the Hellenistic to Late Antiquity [37].

4.2. Between Disconnection and Reconnection: The Transformation History of the Cistern

The disconnectivity related to the cistern's existence is twofold:

(1) The Bir el-Umdan cistern functions as a physical barrier that disconnects the upper and lower reaches of the fluvial stream, significantly altering the natural fluvial processes. The cistern impounds the channel, and the water captured in the cistern is used by the locals, preventing the water from flowing downstream. Thus, similarly to other reservoirs used for agriculture, the water stored in the cistern is stored, accumulated and used by humans mainly to water the herds. The cistern truncates the flood peaks, restricts the discharge, and acts as a sediment trap, capturing the deposits that would otherwise be transported downstream.

(2) Anthropogenic alterations within the drainage basin resulted in the cistern's disconnection from its hydrological catchment during the 20th century until subsequent modifications re-established a connection several decades later. Detailed map analysis reveals this connection–disconnection history of the cistern throughout the evolution of the cistern's cartographic representation (Figure 5). The earliest record of the cistern is in the British 'Survey of Western Palestine' (SWP) map from 1880, which identifies it as Biar el-M'aziyeh. According to the SWP index (sheet XVIII; [49]), this name translates to 'The wells of the M'aziyeh' (goatherd in Arabic) [55]. The map also indicates that the cistern was located in a remote area, devoid of roads or paths. Sixty years later, British Mandate maps from 1935 and 1943 omit the cistern entirely, although a footpath appears, traversing the vicinity. A consecutive map from 1967 [56] does mark the cistern and displays a new road network with a designation text for 'future paving'. Additional data from a British aerial photograph from 1945 (PS; [49]) corroborate the absence of an adjacent road or specific hillside trenches that are seen today, while a contemporary aerial image (2023) clearly delineates both the road and the hillside trenches (Figure 6).

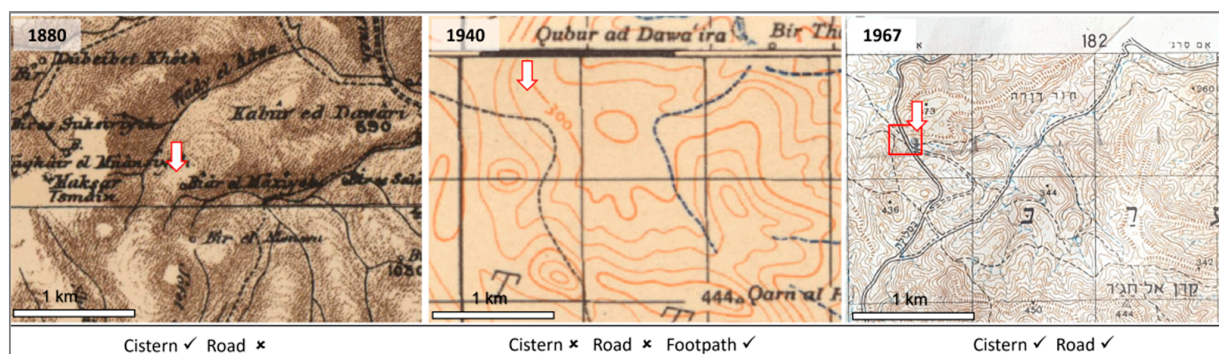


Figure 5. Historical maps illustrating the area of the cistern location (red arrows) and the neighboring road: 1880 [50], 1943 [51], and 1967 [56]. Red square in the 1967 map points on the aerial photo frame in Figure 6b.

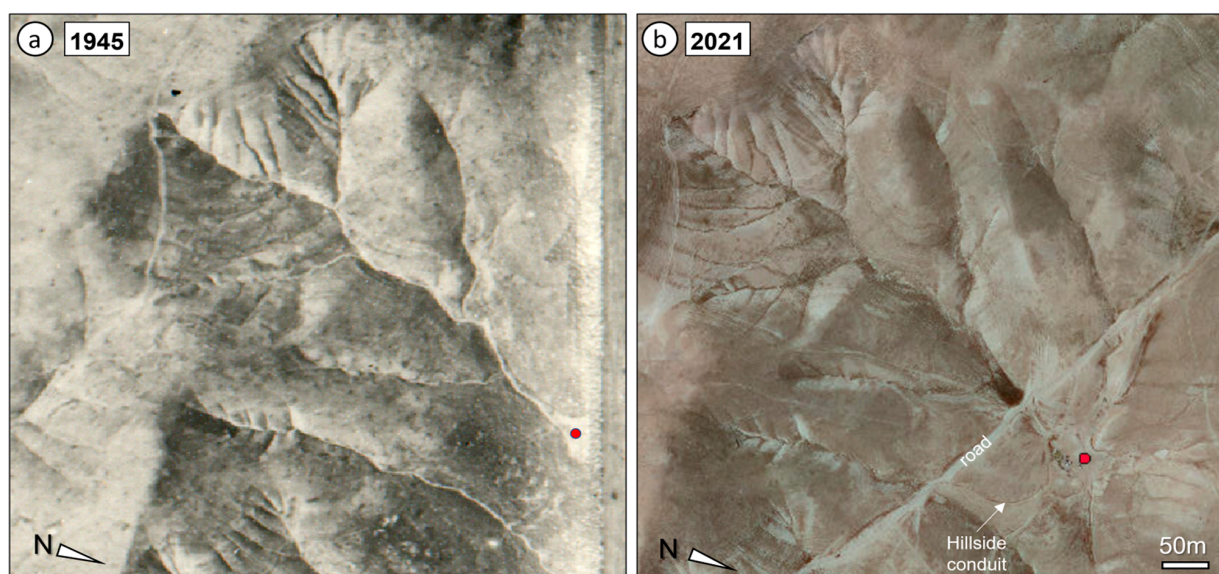


Figure 6. (a) Aerial photo from 1945 (PS; [49]) showing the water cistern location (red dot); (b) aerial photo (2021) of the same location [52], showing the cistern (red dot). Modern constructions are easily identified, including the dirt road, the hillside conduit, and the buildup of an alluvial fan upstream of the road (visible as a darker area in the channel).

The construction of this road, likely initiated in the early 1960s, is pivotal, as it significantly impacted the cistern's hydrology. The road effectively disconnected the cistern from its drainage basin area, reducing the water inflow significantly and potentially resulting in its temporary inoperability. Field evidence supports this claim, noting a renovation in the 2010s that included dredging, cleaning and modern plastering to restore the cistern's functionality. Te'amerah, the Bedouin tribe active in the area, engages occasionally in the maintenance and cleaning of the cistern surroundings.

Despite its current utility, the road lacks underlying drainage pipes, contributing to the cistern's disconnection from its natural catchment. Runoff accumulates upstream of the road, forming a 60 m long alluvial fan and a seasonal shallow pond with increased vegetation (Figures 6 and 7). The alluvial fan and the road obstruct the floods, preventing water from flowing downstream and reaching the cistern. The alluvial fan appears to accommodate small and moderate floods, and overflow across the road might occur only during extreme events. Three gullies developed downstream of the road due to headward erosion (Figure 7). However, as of our 2022 observations, the road remains intact and shows no signs of fluvial entrenchment, probably pointing to a minimal impact of the overflowing water. Subsequently, a hillside conduit was carved along the southern slope, probably

during the cistern renovation in 2010, to supply water by capturing runoff from an adjacent basin. As presented in Figure 1b, these two small basins are distinct and hydrologically separated. The current drainage basin of the cistern, measuring 0.03 km², is only 25% of the natural basins' original size, and as illustrated in Figures 8 and 9, this reduced drainage area is insufficient to fill the cistern annually.



Figure 7. Aerial photo of the cistern area (red arrow). Note the three gully heads that begin by the road due to back-erosion (blue arrows) and the alluvial fan formed upstream (Af), highlighted by increased vegetation. The road and the alluvial fan disconnect the upper and lower reaches of the channel. The road lacks drainage pipes that cross underneath.

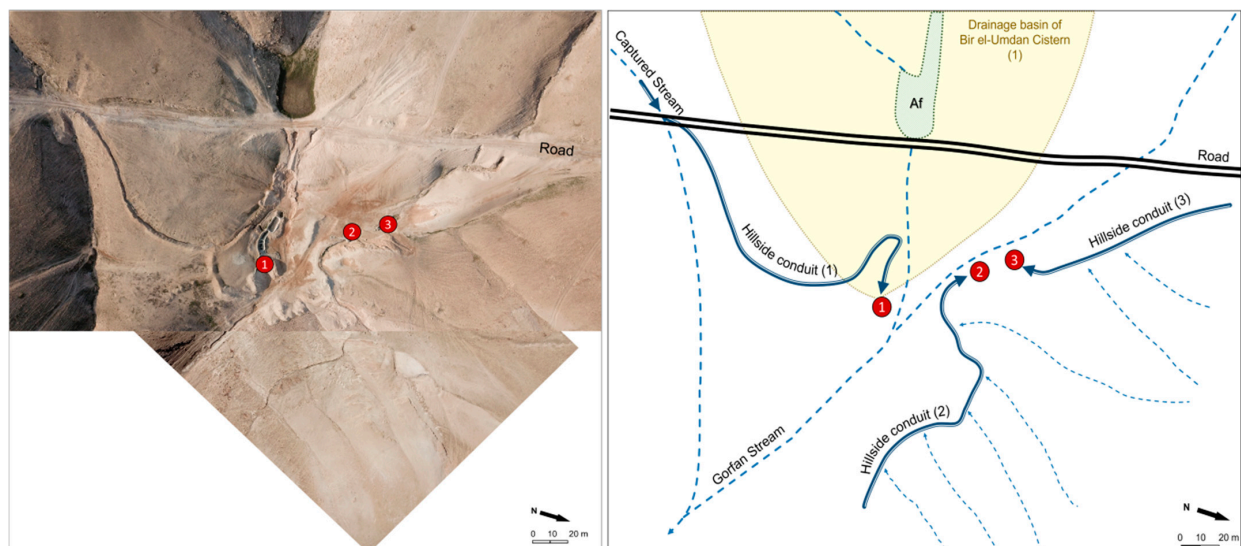


Figure 8. Aerial photo (2022) and map of cistern Bir el-Umdan. The surrounding slopes, and the two nearby and currently inaccessible cisterns (2 and 3). Note the hillside conduits that convey first-order channels into the cisterns. Conduit 1, in particular, captures a southern channel, expanding the catchment area by approximately 25%. Note the alluvial fan, formed by the road, disconnecting cistern 1 from its natural catchment.

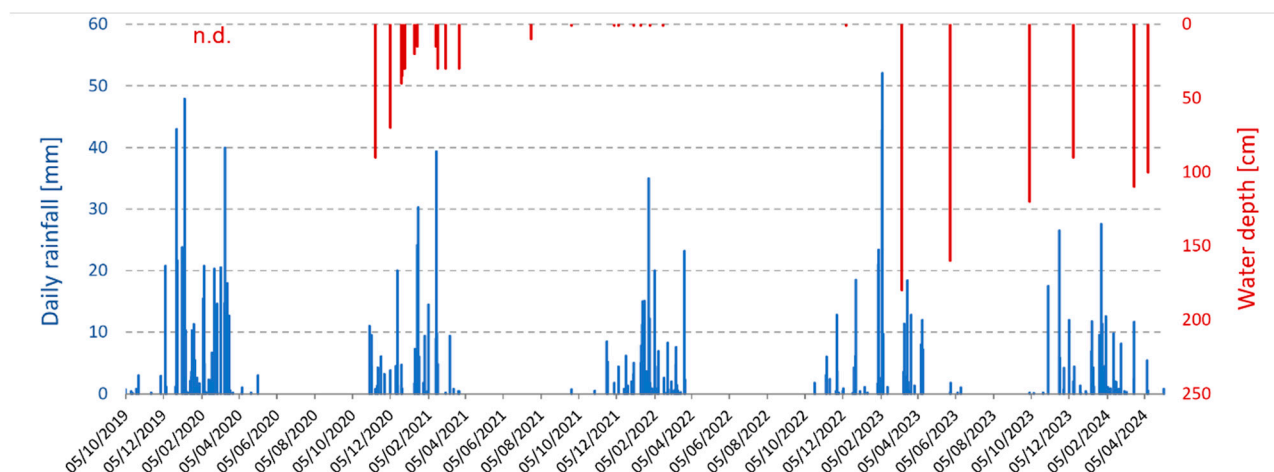


Figure 9. Daily rainfall at Maàle Amos (<https://ims.gov.il/he/ClimateAtlas>, accessed on 1 September 2024) and water depth in the cistern. The water levels represent observations collected by visitors and do not reflect the runoff volume of individual rainfall events. n.d. = no data.

This modification, absent in the British aerial photo from 1945, likely coincided with the renovation of the cistern in the 2010s, proving the need to increase the water volume in the cistern. Additional hillside conduits convey runoff from adjacent slopes to cisterns #2 and #3, constructed in the neighboring basin northwest of the studied cistern (#1). These two cisterns were also disconnected from their active feeding channel by the road. Figure 8 illustrates the current complex water collection system by the hillside conduits in the catchment and the adjacent cisterns.

4.3. Rainfall–Runoff Relations and Water Availability at Bir el-Umdan Cistern

As most of the annual precipitation (~75%) occurs during winter (December to February), the water level measured in the cistern is expected to have a similar trend. Figure 9 summarizes the daily rainfall distribution in the nearby Maàle Amos station for 2019–2024. In addition, since 2020, increased local visits to the site have produced reliable data on its water levels. First observations at the end of 2020 indicated that the water level in the cistern ranged from 50 to 70 cm, most likely a remnant of floodwater from the previous rainy season. The water level did not rise significantly during the next season despite two rainfall events of 40 mm/day. By the summer of 2021, the cistern had completely dried up and remained dry throughout the rainy season of 2021/2022, as confirmed by eight separate observations. A severe rainfall event on 7 February 2023 resulted in the rapid filling of the cistern. Subsequent visits by hikers on 10 March 2023 revealed a water level of 1.8 m, which continued to recede over the following summer. In January 2024, another event resulted in an increase of about 20 cm in the water level, observed approximately two months later.

The runoff coefficient, or the ratio of the water volume in the cistern to the total volume of precipitation during a certain event, was calculated for four instances where visitor observations closely coincided with rainfall events and where it was clear that the rise in the cistern’s water level was directly attributable to the rainfall event (Table 1). The formula used to calculate the runoff coefficient is:

$$C_c = V_c / (R_c * A) * 100 \quad (1)$$

where:

- C_c is the runoff coefficient caught by the cistern (%);
- V_c is the water volume in the cistern (m^3);
- R_c is the rainfall depth at the study site (mm);
- A is the catchment size (0.03 km^2).

Table 1. Four flood events trapped by the cistern and Runoff Coefficient (RC). * Calculated as 25% less than rainfall at Ma'ale Amos. ** The hillside conduit drainage basin = 0.03 km².

Date	Rainfall at Ma'ale Amos [mm]	Rainfall at Cistern [mm] *	Δ Volume in Cistern [m ³]	Rainfall Volume [m ³] **	RC Caught by Cistern [%]
17–18 February 2021	49.3	39.5	17	1185	1.4
6–8 February 2023	105	84	205	2520	8.1
26–28 January 2024	40.4	32.3	25	970	2.6
23–27 February 2024	50.5	40.4	23	1212	1.9

It is important to note that our calculations are based on estimated rainfall amounts due to the lack of specific rainfall data measured at the study site. Daily rainfall amounts at Ma'ale Amos were adjusted and normalized to the cistern area, but other important factors, such as rainfall duration and intensity, soil properties, antecedent soil moisture, or the presence of crusts, remain unknown. Also, it is assumed that all the drainage basin area received the same rainfall amount, which is a considerable assumption for such a small basin. Therefore, these calculations should be considered an upper limit.

4.4. Soil Erosion and Sedimentation Basin Efficiency

To analyze the eroded sediment entering the cistern, soil samples were collected from the slope, and infill sediment was retrieved from the six upstream sedimentation basins and the bottom of the cistern (Figure 10). The soils over the slopes are shallow, ~10 cm thick, light yellowish brown (10YR 6/3), and stony (40–70%). The coarse fraction consists of sub-angular to sub-rounded fragments of chalk and chert from the Mishash Formation and pyrometamorphic gravels derived from the Hatrurim Formation, 3–10 cm in diameter.

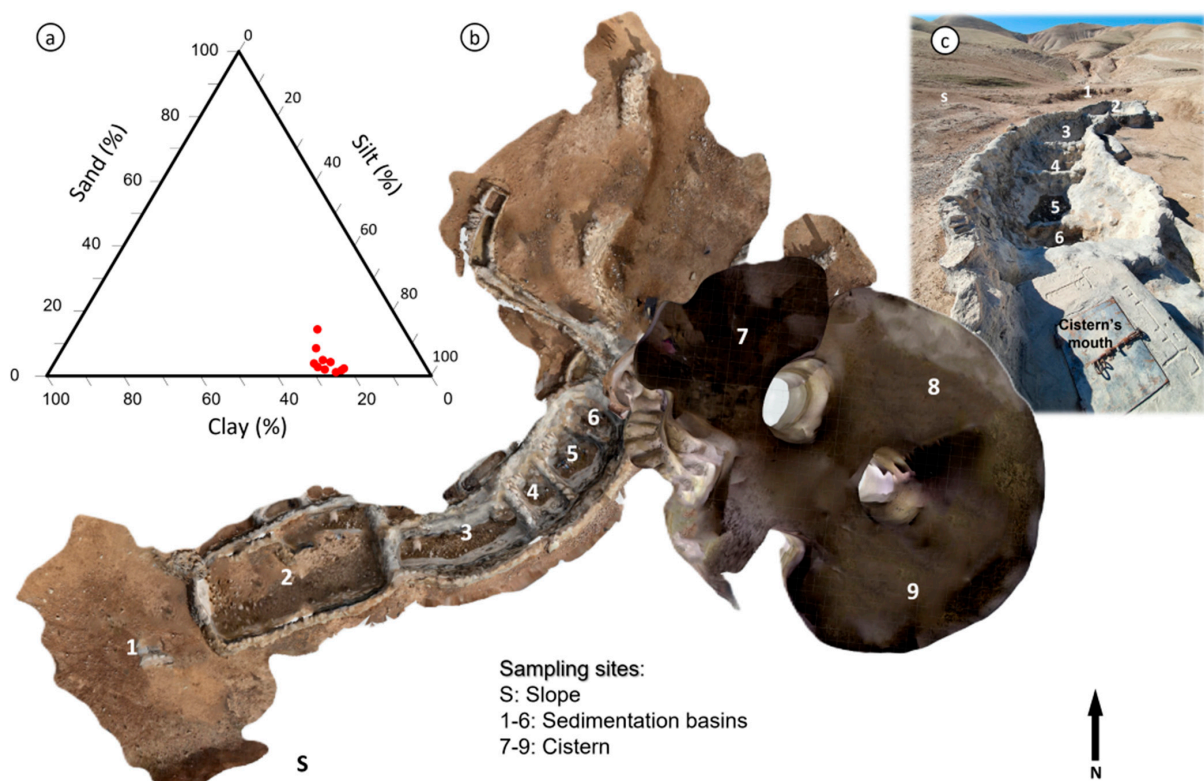


Figure 10. Sediment samples were collected from the slope (s), the sedimentation basins (1–6) and from the cistern (7–9). (a) Grain size distribution; (b) Lidar imaging of the sedimentation basins and the cistern. Three-dimensional scan prepared by Dr. Danny Bickson; (c) land photo of the sedimentation basins.

The fine fraction is dominated by silt (65–75%), with 22–30% clay and limited quantities of sand (2–5%). A comparison of the sediment sampled from the slope, sedimentation basins, and cistern bottom revealed high similarity (Figure 10). The minimal variations observed between the samples suggest that suspended sediment is rapidly transported into the cistern during the flood, without settling time for sedimentation. Except for sedimentation basins 5 and 6, which exhibited higher percentages of sand (8.6% and 14.4%, respectively), there were no significant differences among the samples from the different sedimentation basins. This increase in sand fraction is likely attributed to suspended organic matter (primarily goat droppings and dry branches). Trapped by the filter net at the cistern's entrance, the materials accumulated in the last two sedimentation basins.

5. Discussion

In arid environments, developing water collection and storage techniques has always been crucial in supporting human life. One effective strategy to address water scarcity was the construction of reservoirs and cisterns to capture surface runoff during infrequent rainfall events. These structures, including both open reservoirs and rock-cut cisterns, are prevalent throughout the Judean Desert and the arid Negev Highlands [57]. Along with two other adjacent rock-cut cisterns, Bir el-Umdan is highlighted as one of the largest and most impressive water systems in the Judean Desert. It includes an external construction of sedimentation basins for diverting the water and facilitating sedimentation and a large underground chamber reaching a capacity of $\sim 700\text{ m}^3$ for water storage.

5.1. The Cistern's History of Disconnectivity and Reconnectivity

The cistern was likely constructed in antiquity, but the exact age is uncertain due to renovations in the 2010s and the elimination of remaining archaeological artifacts. Historical records of the cistern are limited to maps and contemporary accounts beginning in the 19th century. The oldest known map, the 1880 Survey of Western Palestine, labels the cistern as "Biar el-Māziyeh" or "The wells of the goat herds." Surprisingly, it is absent from subsequent British Mandate maps (1935, 1943) and only reappears on a 1967 Israeli map which may indicate the cistern's disuse or blockage during this intermediate period. The construction of a road approximately 80 m upstream from the cistern during the 1960s dramatically affected its water and sediment balance, as it totally disconnected the cistern from its natural drainage basin, blocking floodwaters and sediment from transporting downstream. The flood waters were impounded upstream of the road and did not continue downslope; the sediment was retained in the channel, and, as a result, in the last 55 years, an alluvial fan bounded by the road gradually accumulated above the cistern. The site history remains unclear until the 2010s, when the cistern underwent a significant renovation, including cleaning, repairing, and applying a new, modern plaster coating. In addition, six sedimentation basins were constructed upstream to filter out sediments and improve the water quality reaching the cistern.

While small and moderate winter floods are now accommodated upstream in the alluvial fan, exceptional events can still overflow the road barrier and reach the cistern. To increase surface runoff, a hillside conduit was entrenched along the slopes to collect water from the southern channel and divert it into the cistern. Although this conduit drains only a limited area of 0.03 km^2 , it has reconnected the cistern to the slopes, allowing only its partial fill. Hillside conduits were also built for the two neighboring cisterns, visible from both land and aerial photos, to address the same water supply deficit caused by the road.

5.2. Rainfall–Runoff Relations and Water Availability

The significant investment in constructing such a large cistern (which peaks at $\sim 700\text{ m}^3$) seems disproportional to its current relatively small water capacity. However, the cistern's observed water levels over the past 15 years are derived from a small (0.03 km^2) drainage basin, which equals a quarter of the original natural basin, suggesting that by the time of construction, the cistern had access to considerably larger water volumes, deriving from a

vaster drainage basin. We analyzed the 21st-century runoff coefficient and recurrence interval over the original drainage basin (0.12 km^2) to estimate the water volumes in antiquity. The runoff coefficients obtained for the water volume in the cistern are between 1.4% and 8.1%, which are generally lower than those reported in other desert regions. Studies on runoff in small basins in the Negev desert [58] have found average runoff rates of approximately 10%, while Eldridge et al. [59] reported rates ranging from 6% to 32% in disturbed and undisturbed regions, respectively, depending on crust and vegetation conditions.

To estimate potential water volumes during the cistern's construction period, we analyzed the runoff coefficient obtained for the 21st-century volumes and plotted its recurrence interval over the natural drainage basin area (0.12 km^2), representing the area before the road construction (Figure 11). Based on the highest watermarks observed on the cistern walls, the most significant infill event within the past 15 years resulted in a total cistern volume of 285 m^3 , suggesting a recurrence interval of approximately 15 years. Moreover, the largest recorded event (6–8 February 2023), with 84 mm of rainfall, yielded a cistern volume of 205 m^3 . This event appears to occur every seven years when plotted on the recurrence interval line. By extrapolating the runoff coefficient (8.1% for the 0.03 km^2 basin area) to the original, natural basin size, we can estimate a potential water volume of 806 m^3 , implying a cistern overflow every 6–7 years. Although possible, this value seems excessively infrequent. A more conservative estimate using a runoff coefficient of 5% yields a water volume of approximately 500 m^3 , corresponding to a recurrence interval of seven years and a potential overflow once every 15 years.

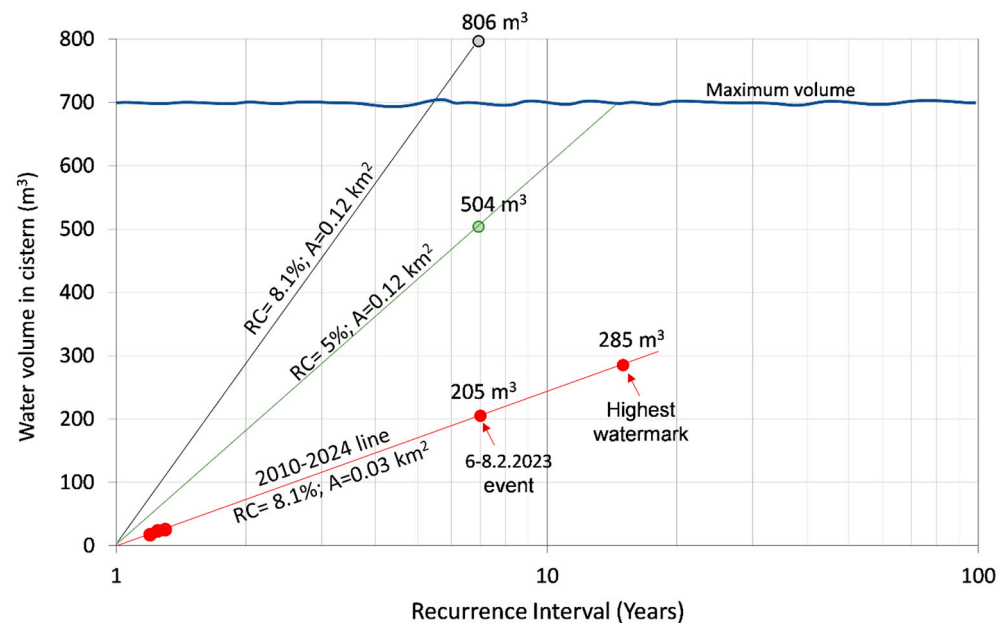


Figure 11. Evaluation of water volume potential at the original drainage basin size, based on the runoff coefficient obtained for an event with a seven-year recurrence interval.

5.3. Soil Erosion and Sedimentation Basin Efficiency

The drainage basin of the Bir el-Umdan cistern, like most others in the Judean Desert, is significantly affected by grazing. Near-zero vegetation cover exposes the entire hillslope surface to the pressure of sheep and goats, leading to increased raindrop impact and splash erosion, accelerated aggregate breakdown, soil compaction from trampling, and the formation of physico-chemical and biogenic crusts over large areas. These factors contribute to high rates of Hortonian overland flow and erosion due to runoff continuity over relatively long distances [60]. Thus, rainfall in the Judean Desert leads to flash floods with high sediment transport rates, displaying short, intense rainstorms and infrequent floods, resulting in complex rainfall–runoff relations [61].

As the cistern is situated within the channel, it is fed by floodwaters and prone to high sedimentation. The sedimentation history within the cistern and the external basins is challenging to reconstruct due to potential dredging operations conducted since the cistern's renovation. These operations may have obscured the true extent of sediment accumulation. However, sediment analysis of the slopes, sedimentation basins, and cistern bottom revealed a high similarity in the sediment's physical characteristics, suggesting rapid water flow during flood events with no settling time for sedimentation. The sediment accumulated in the water system is similar to the fine fraction of the soils over the adjacent slopes. Few gravels transported by saltation were found in the sedimentation basins.

The cistern's disconnection from its natural drainage basin and subsequent reconnection to a smaller basin significantly impacted its function. To better understand the effects of these changes, further research on sediment transport volumes and accumulation rates is needed. In this manner, the upstream alluvial fan may provide valuable insights into historical flow patterns and sediment entry into the system. By analyzing the characteristics of the alluvial fan, future research could potentially reconstruct the cistern's past sedimentation dynamics and assess the long-term impacts of the changes in a small, impounded arid drainage basin.

6. Conclusions

The Bir el-Umdan cistern, a significant archaeological site in the Judean Desert, has attracted considerable public attention since 2020. The cistern is part of a larger water system that includes two other nearby cisterns, together forming one of the most remarkable water systems in the region. This impressive structure is estimated to date back to the Hellenistic to Late Antiquity periods, based on its architectural characteristics. Excavated in chalk, the cistern has a capacity of $\sim 700 \text{ m}^3$. Two imposing columns, each with a base diameter of 2.5 m, support the ceiling within the cistern's interior.

The cistern was initially documented on 19th-century SWP map but was subsequently omitted from British Mandate maps. It reappeared on the 1967 Survey of Israel map, including an upstream road that was likely constructed in the 1960s. This road cut the cistern's connection to its natural drainage basin. In the 2010s, the cistern underwent restoration and renovation and was reconnected via a hillside conduit to a smaller drainage basin, constituting only 25% of the original one. Consequently, the water supply remains limited.

The runoff coefficients calculated for the cistern's drainage basin are relatively low (1.4–8.1%), compared to other documented desert basins (10% or higher). To estimate past water volumes, we used the 21st-century runoff coefficient and recurrence interval over the original drainage basin (0.12%). Using an 8.1% runoff coefficient, the estimated water volume is 806 m^3 , implying a cistern overflow every 6–7 years. A more conservative runoff coefficient of 5% yields an estimated water volume of 500 m^3 and a 15-year recurrence interval.

This research is subject to several limitations. (1) The nearest rain gauge is located within a slightly different climatic zone, receiving approximately 25% more annual rainfall. This introduces uncertainty when correlating rainfall events over the small inverted catchment with the recorded data. While we assume a general correlation, we account for this difference by reducing the recorded rainfall by 25% for each event. (2) The water level in the cistern was estimated based on visual observations. Although we are confident in the timing of these observations, the exact water level may vary slightly due to irregularities in the cistern's bottom. This leads to a less precise estimation of water levels. (3) The relatively small number of observations, spanning only four years, limits the statistical power of our analysis and may constrain the generalizability of our findings.

The cistern's location within the channel and its floodwater source makes the cistern prone to high rates of sedimentation. However, due to maintenance and possible dredging operations, reconstructing sediment accumulation remains a significant challenge. Silt particles dominate the sediment accumulated in both cistern and sedimentary basins, and the consistent grain size distribution throughout the system indicates rapid water flow

during flood events. Further research on sediment transport and accumulation rates is necessary to fully understand the long-term impacts of the drainage basin changes and inform future management strategies in arid regions, both locally and globally.

Author Contributions: Conceptualization, N.S.-Z. and B.Z.; Methodology, N.S.-Z. and B.Z.; Investigation, N.S.-Z. and B.Z.; Resources, N.S.-Z. and B.Z.; Writing—original draft, N.S.-Z. and B.Z.; Writing—review & editing, N.S.-Z. and B.Z. All authors have read and agreed to the published version of the manuscript.

Funding: This research received no external funding.

Data Availability Statement: The original contributions presented in the study are included in the article, further inquiries can be directed to the corresponding author.

Acknowledgments: We gratefully acknowledge Hilit Kranenburg for her assistance with lab analysis and Danny Bickson for the Lidar scanning and imaging of the cistern, both of which were crucial to this study.

Conflicts of Interest: The author declares no conflicts of interest.

References

1. Saco, P.M.; Rodríguez, J.F.; Moreno-de las Heras, M.; Keesstra, S.; Azadi, S.; Sandi, S.; Baartman, J.; Rodrigo-Comino, J.; Rossi, M.J. Using hydrological connectivity to detect transitions and degradation thresholds: Applications to dryland systems. *Catena* **2020**, *186*, 104354. [\[CrossRef\]](#)
2. Bracken, L.J.; Croke, J. The concept of hydrological connectivity and its contribution to understanding runoff-dominated geomorphic systems. *Hydrol. Process* **2007**, *21*, 1749–1763. [\[CrossRef\]](#)
3. Poepl, R.E.; Keesstra, S.D.; Maroulis, J. Conceptual connectivity framework for understanding geomorphic change in human-impacted fluvial systems. *Geomorphology* **2017**, *277*, 237–250. [\[CrossRef\]](#)
4. Keesstra, S.; Nunes, J.P.; Saco, P.; Parsons, T.; Poepl, R.; Masselink, R.; Cerdà, A. The way forward: Can connectivity be useful to design better measuring and modelling schemes for water and sediment dynamics? *Sci. Total Environ.* **2018**, *644*, 1557–1572. [\[CrossRef\]](#)
5. Khan, S.; Fryirs, K.; Bizzi, S. Modelling sediment (dis) connectivity across a river network to understand locational-transmission-filter sensitivity for identifying hotspots of potential geomorphic adjustment. *Earth Surf. Proc. Land.* **2021**, *46*, 2856–2869. [\[CrossRef\]](#)
6. Ayer, J.E.B.; Lämmle, L.; Mincato, R.L.; Donadio, C.; Avramidis, P.; Pereira, S.Y. Three-dimensional model and environmental fragility in the Guarani Aquifer system, SE-Brazil. *Groundw. Sustain. Dev.* **2024**, *26*, 101285. [\[CrossRef\]](#)
7. Wohl, E. Connectivity in rivers. *Prog. Phys. Geog* **2017**, *41*, 345–362. [\[CrossRef\]](#)
8. Yair, A.; Lavee, H.; Kossovsky, A.; Yassif, N.R.; Goldsheger, N. Complex hydrological regimes and processes, in the Negev arid area, Israel. *Earth Environ. Sci. Res. Rev.* **2024**, *7*, 1–12.
9. Millares-Valenzuela, A.; Eekhout, J.P.; Martínez-Salvador, A.; García-Lorenzo, R.; Pérez-Cutillas, P.; Conesa-García, C. Evaluation of sediment connectivity through physically-based erosion modeling of landscape factor at the event scale. *Catena* **2022**, *213*, 106165. [\[CrossRef\]](#)
10. Ondráčková, L.; Máčka, Z. Geomorphic (dis) connectivity in a middle-mountain context: Human interventions in the landscape modify catchment-scale sediment cascades. *Area* **2019**, *51*, 113–125. [\[CrossRef\]](#)
11. Poepl, R.E.; Polvi, L.E.; Turnbull, L. (Dis) connectivity in hydro-geomorphic systems—emerging concepts and their applications. *Earth Surf. Proc. Land.* **2023**, *48*, 1089–1094. [\[CrossRef\]](#)
12. Xingyuan, Z.; Fawen, L.; Yong, Z. Impact of changes in river network structure on hydrological connectivity of watersheds. *Ecol. Indic.* **2023**, *146*, 109848. [\[CrossRef\]](#)
13. Magilligan, F.J.; Graber, B.E.; Nislow, K.H.; Chipman, J.W.; Sneddon, C.S.; Fox, C.A. River restoration by dam removal: Enhancing connectivity at watershed scales. *Elementa* **2016**, *4*, 000108. [\[CrossRef\]](#)
14. Dépret, T.; Riquier, J.; Piégay, H. Evolution of abandoned channels: Insights on controlling factors in a multi-pressure river system. *Geomorphology* **2017**, *294*, 99–118. [\[CrossRef\]](#)
15. Roy, S. Transportation Infrastructure and Geomorphic Connectivity. In *Disturbing Geomorphology by Transportation Infrastructure*; Earth and Environmental Sciences Library; Springer: Cham, Switzerland, 2023. [\[CrossRef\]](#)
16. Poepl, R.E.; Fryirs, K.A.; Tunnicliffe, J.; Brierley, G.J. Managing sediment (dis)connectivity in fluvial systems. *Sci. Total Environ.* **2020**, *736*, 13962. [\[CrossRef\]](#)
17. James, L.A.; Lecce, S.A. Impacts of land-use and land-cover change on river systems. In *Treatise on Fluvial Geomorphology*; Wohl, E., Ed.; Elsevier: Amsterdam, The Netherlands, 2013; pp. 768–793.
18. Caschetto, M.; Barbieri, M.; Galassi, D.M.; Mastroiello, L.; Rusi, S.; Stoch, F.; Di Cioccio, A.; Petitta, M. Human alteration of groundwater–surface water interactions (Sagittario River, Central Italy): Implication for flow regime, contaminant fate and invertebrate response. *Environ. Earth Sci.* **2014**, *71*, 1791–1807. [\[CrossRef\]](#)

19. Bar-Yosef, O. Prehistory of the Levant. *Annu. Rev. Anthr.* **1980**, *9*, 101–133. Available online: <https://www.jstor.org/stable/2155731> (accessed on 1 September 2024). [CrossRef]
20. Bar-Adon, P.; Greenhut, Z. Excavations in the Judean Desert. *Atiqot Hebr. Ser.* **1989**, *9*, 1–8.
21. Davidovich, U. The chalcolithic-early bronze age transition: A view from the Judean Desert Caves, Southern Levant. *Paléorient* **2013**, *39*, 125–138. Available online: <https://www.jstor.org/stable/43576767> (accessed on 1 September 2024). [CrossRef]
22. Goren, Y. Gods, caves, and scholars: Chalcolithic cult and metallurgy in the Judean Desert. *Near East. Archaeol.* **2014**, *77*, 260–266. [CrossRef]
23. Harel, M. Israelite and Roman Roads in the Judean Desert. *Isr. Explor. J.* **1967**, *17*, 18–26. Available online: <https://www.jstor.org/stable/27925078> (accessed on 1 September 2024).
24. Zissu, B. Kings, Hermits, and Refugees in the Judean Desert in the Late Second Temple Period and at the Time of the Bar-Kokhba Revolt. In *New Studies in the Archaeology of the Judean Desert*; Sion, O., Uziel, J., Ganor, A., Klein, E., Eds.; The Israel Antiquities Authority: Jerusalem, Israel, 2023.
25. Porath, Y. *The Synagogue at En-Gedi*; Qedem 64; The Hebrew University: Jerusalem, Israel, 2022.
26. Porat, R. The Physical Conditions and Road Network between Ein Gedi and Qumran. In *The Refuge Caves from the Period of the Bar-Kokhba Revolt*; Eshel, H., II, Porat, R., Eds.; Israel Exploration Society and Jeselsohn Epigraphic Center of Jewish History: Jerusalem, Israel, 2009; pp. 10–27. (In Hebrew)
27. Bruins, H.J.; Evenari, M.; Nessler, U. Rainwater-harvesting agriculture for food production in arid zones: The challenge of the African famine. *Appl. Geogr.* **1986**, *6*, 13–32. [CrossRef]
28. Ilan, S. Ancient Waterworks in the Judean Desert. In *The Judean Desert and the Dead Sea*; Ilan, S., Ed.; Society for the Protection of Nature: Tel Aviv, Israel, 1973; pp. 385–389. (In Hebrew)
29. Lavee, H.; Poesen, J.; Yair, A. Evidence of high efficiency water-harvesting by ancient farmers in the Negev Desert, Israel. *J. Arid. Environ.* **1997**, *35*, 341–348. [CrossRef]
30. Bruins, H.J. Ancient desert agriculture in the Negev and climate-zone boundary changes during average, wet and drought years. *J. Arid. Environ.* **2012**, *86*, 28–42. [CrossRef]
31. Ackermann, O.; Zhevelev, H.M.; Svoray, T. Agricultural systems and terrace pattern distribution and preservation along climatic gradient: From sub-humid Mediterranean to arid conditions. *Quat. Int.* **2019**, *502*, 319–326. [CrossRef]
32. Stager, L.E. Farming in the Judean desert during the Iron Age. *Bull. Am. Sch. Orient. Res.* **1976**, *221*, 145–158. [CrossRef]
33. Langgut, D.; Neumann, F.H.; Stein, M.; Wagner, A.; Kagan, E.J.; Boaretto, E.; Finkelstein, I. Dead Sea pollen record and history of human activity in the Judean Highlands (Israel) from the Intermediate Bronze into the Iron Ages (~2500–500 BCE). *Palynology* **2014**, *38*, 280–302. [CrossRef]
34. Gibson, S.; Lewis, R.Y.; Taylor, J.E. The Bugeica Plateau of the Judean Desert in the Southern Levant During the Seventh to Early Sixth Centuries BCE: Iron Age Run-off Farmland or a Pastoralist Rangeland? In *“And in Length of Days Understanding” (Job 12:12): Essays on Archaeology in the Eastern Mediterranean and Beyond in Honor of Thomas E. Levy*; Ben-Yosef, E., Jones, I.W.N., Eds.; Springer International Publishing: Cham, Switzerland, 2023; pp. 839–897. [CrossRef]
35. Ben-Yosef, T. *The New Israel Guide: The Judean Desert and Dead Sea Valley*; Society for the Protection of Nature in Israel: Jerusalem, Israel, 2001; Volume 13. (In Hebrew)
36. Lavee, H. A Climatic Eco-geomorphological Transect Across the Major Climatic Belts of Israel—Processes, Patterns, and Desertification. In *Landscapes and Landforms of Israel*; World Geomorphological Landscapes; Frumkin, A., Shtober-Zisu, N., Eds.; Springer: Cham, Switzerland, 2024; pp. 207–222. [CrossRef]
37. Klöner, A. Water cisterns in Idumaea, Judaea and Nabatea in the Hellenistic and early Roman periods. *Binos Actus Lumina* **2005**, *2*, 129–148.
38. Fryirs, K.A.; Brierley, G.J.; Preston, N.J.; Kasai, M. Buffers, barriers and blankets: The (dis) connectivity of catchment-scale sediment cascades. *Catena* **2007**, *70*, 49–67. [CrossRef]
39. Mor, U.; Burg, A. Geological Map of Israel 1:50,000. *Mitzpe Shalem* **2000**. Sheet 12-III.
40. Geller, Y.I.; Burg, A.; Halicz, L.; Kolodny, Y. System closure during the combustion metamorphic “Mottled Zone” event, Israel. *Chem. Geol.* **2012**, *334*, 25–36. [CrossRef]
41. Arkin, Y.; Ecker, A. *Geotechnical and Hydrogeological Concerns in Developing the Infrastructure Around Jerusalem*; Geological Survey of Israel: Jerusalem, Israel, 2007.
42. Shtober-Zisu, N.; Zissu, B. Lithology and the distribution of Early Roman-era tombs in Jerusalem’s necropolis. *Prog. Phys. Geog* **2018**, *42*, 628–649. [CrossRef]
43. Dayan, U.; Morin, E. Flash flood-producing rainstorms over the Dead Sea: A review. In *New Frontiers in Dead Sea Paleoenvironmental Research*; Enzel, Y., Agnon, A., Stein, M., Eds.; GSA. Sp. Paper; The Geological Society of America Special Paper 401: Boulder, CO, USA, 2006. [CrossRef]
44. Greenbaum, N.; Ben-Zvi, A.; Haviv, I.; Enzel, Y. The hydrology and paleohydrology of the Dead Sea tributaries. In *New Frontiers in Dead Sea Paleoenvironmental Research*; Enzel, Y., Agnon, A., Stein, M., Eds.; GSA. Sp. Paper; The Geological Society of America Special Paper 401: Boulder, CO, USA, 2006. [CrossRef]
45. Knippertz, P. Tropical–extratropical interactions associated with an Atlantic tropical plume and subtropical jet streak. *Mon. Weather. Rev.* **2005**, *133*, 2759–2776. [CrossRef]

46. Zituni, R.; Greenbaum, N.; Porat, N.; Benito, G. Magnitude, frequency and hazard assessment of the largest floods in steep, mountainous bedrock channels of the Southern Judean Desert, Israel. *J. Hydrol.* **2021**, *37*, 100886. [CrossRef]
47. Steinberger, Y.; Lavee, H.; Barness, G.; Davidor, M. Soil carbohydrates along a topoclimatic gradient in a Judean desert ecosystem. *Land. Degrad. Dev.* **1999**, *10*, 523–530. [CrossRef]
48. Danin, A.; Fragman-Sapir, O. Flora of Israel and Adjacent Areas. 2016. Available online: <https://flora.org.il/en/plants/> (accessed on 1 September 2024).
49. Royal Air Force Squadron 680, Great Britain 1945, PS22: 5039. [Aerial Photograph].
50. Conder, C.R.; Kitchener, H.H. *The Survey of Western Palestine; Memoirs of the Topography, Orography, Hydrography, and Archaeology; Palestine Exploration Fund: London, UK, 1883; Volume III: Sheets XVII–XXVI.*
51. Survey of Palestine. 1943. Ein Et Turaba, 1:20,000 [Map].
52. Survey of Israel. 2024. Available online: <http://govmap.co.il> (accessed on 1 September 2024).
53. Israel Meteorological Service. *Clim. Atlas*. 2024. Available online: <https://ims.gov.il/he/ClimateAtlas> (accessed on 1 September 2024).
54. Soil Science Division Staff. *Soil Survey Manual, USDA Handbook 18; Department of Agriculture (USDA): Washington, DC, USA, 2017.*
55. Stewardson, H.C. *The Survey of Western Palestine: A General Index; Committee of the Palestine Exploration Fund: London, UK, 1888.*
56. Survey of Israel. 1967. Ein Et Turaba, 1:50,000 [Map 2-A-50-12/III-1967].
57. Junge, A.; Lomax, J.; Shahack-Gross, R.; Finkelstein, I.; Fuchs, M. Chronology of an ancient water reservoir and the history of human activity in the Negev Highlands, Israel. *Geoarchaeology* **2018**, *33*, 695–707. [CrossRef]
58. Bruins, H.J.; Bithan-Guedj, H.; Svoray, T. GIS-based hydrological modelling to assess runoff yields in ancient-agricultural terraced wadi fields (central Negev desert). *J. Arid. Environ.* **2019**, *166*, 91–107. [CrossRef]
59. Eldridge, D.J.; Zaady, E.; Shachak, M. Microphytic crusts, shrub patches and water harvesting in the Negev Desert: The Shikim system. *Landsc. Ecol.* **2002**, *17*, 587–597. [CrossRef]
60. Cerdà, A.; Lavee, H. The effect of grazing on soil and water losses under arid and Mediterranean climates, Implications for desertification. *Pirineos* **1999**, *153–154*, 159–174. [CrossRef]
61. Cohen, H.; Laronne, J.B. High rates of sediment transport by flashfloods in the Southern Judean Desert, Israel. *Hydrol. Process* **2005**, *19*, 1687–1702. [CrossRef]

Disclaimer/Publisher’s Note: The statements, opinions and data contained in all publications are solely those of the individual author(s) and contributor(s) and not of MDPI and/or the editor(s). MDPI and/or the editor(s) disclaim responsibility for any injury to people or property resulting from any ideas, methods, instructions or products referred to in the content.